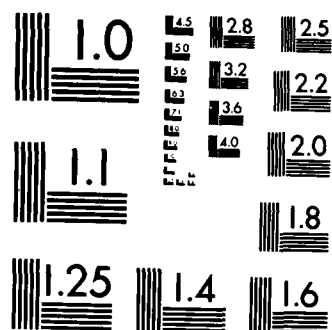MICROCOPY RESOLUTION TEST CHART

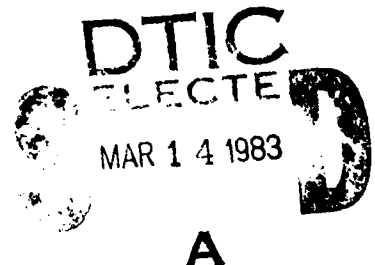NATIONAL BUREAU OF STANDARDS-1963-A

Investigations of Vacuum Ultraviolet

and Soft X-Ray Lasers

Report for

Contract Period 1981 - 1982

by

K. Drühl

Principal Investigator

Marlan O. Scully

Co Principal Investigator

Weng Chow

Institute for Modern Optics
Department of Physics and Astronomy
University of New Mexico
Albuquerque, New Mexico 87131

DTIC
ELECTE
MAR 1 4 1983

A

83 03 14 020

REPORT DOCUMENTATION PAGE		READ INSTRUCTIONS BEFORE COMPLETING FORM
1. REPORT NUMBER AFOSR-TR- 83-0054	**2. GOVT ACCESSION NO.**	**3. RECIPIENT'S CATALOG NUMBER**
4. TITLE *(and Subtitle)* Investigations of Vacuum Ultraviolet and Soft X-Ray Lasers		**5. TYPE OF REPORT & PERIOD COVERED** Annual report 5/15/81 - 5/14/82
		6. PERFORMING ORG. REPORT NUMBER
7. AUTHOR(s) Kai Drühl, Weng W. Chow and Marlan O. Scully		**8. CONTRACT OR GRANT NUMBER(s)** AFOSR-81-0128
9. PERFORMING ORGANIZATION NAME AND ADDRESS Institute for Modern Optics Dept. of Physics and Astronomy Univ. of NM, Albuquerque, NM 87131		**10. PROGRAM ELEMENT, PROJECT, TASK AREA & WORK UNIT NUMBERS** 61102F 2301/A8
11. CONTROLLING OFFICE NAME AND ADDRESS Airforce Office of Scientific Research (AFSC) Bolling AFB, DC 20332		**12. REPORT DATE** November, 1982
		13. NUMBER OF PAGES 29
14. MONITORING AGENCY NAME & ADDRESS*(if different from Controlling Office)*		**15. SECURITY CLASS. (of this report)** Unclassified
		15a. DECLASSIFICATION/DOWNGRADING SCHEDULE

16. DISTRIBUTION STATEMENT *(of this Report)*

Approved for public release;
distribution unlimited.

17. DISTRIBUTION STATEMENT *(of the abstract entered in Block 20, if different from Report)*

18. SUPPLEMENTARY NOTES

19. KEY WORDS *(Continue on reverse side if necessary and identify by block number)*
Charge-exchange, X-ray lasers.

20. ABSTRACT *(Continue on reverse side if necessary and identify by block number)*
A kinematical model which incorporates charge exchange, electron impact ionization of target and plasma screening was developed for a clashing beam charge exchange x-ray laser. Analytic results were obtained, which lead to a better understanding of the basic physical mechanisms and their dependence on cross sections and initial conditions.

UNCLASSIFIED

DD _{1 JAN 73} **1473** EDITION OF 1 NOV 65 IS OBSOLETE
S/N 0102-014-6601 |

I. Introduction

Our work, for the contracted period, was mainly concerned with a theoretical analysis of the clashing beam charge exchange laser. Although this scheme for an X-ray laser was proposed more than ten years ago [1, 2, 3, 4], a careful analysis shows that the pumping kinematics of this laser scheme has not been fully understood. This is due to two related difficulties.

Firstly the rate equations describing the pumping kinematics are quite complex, if they are to include the most important competing processes besides charge exchange itself. For this reason results published so far were derived from numerical solutions [5, 6]. While numerical analysis certainly produces a unique result for any fixed set of paramenters, this result may be difficult to interpret in physical terms without a clear understanding of the underlying physical mechanisms. In fact, we shall show below that physical interpretations given in the literature so far are to a large extent misleading.

The second difficulty is the fact that basic parameters like the charge exchange cross section remain quite uncertain. The standard reference to the latter used to be the theoretical work by Olson and Smith [7]. Recent experimental and theoretical results, however, are in strong disagreement with their predictions [8]. Similar uncertainties, if not as grave, are found for other cross sections of other important processes, like electron impact ionization.

For these reasons we have adopted a two-fold strategy. Our first aim was to reduce the set of rate equations in such a way as

to still give a realistic model on the one hand and to allow for analytical treatment on the other. This goal has been achieved. We have constructed a kinematical model which incorporates charge exchange, electron impact ionization of target, and plasma screening. A similar model results from reducing the rate equations of Copeland, Mahr and Tang [6]. The latter model does not, however, incorporate plasma screening, and leads to violation of space charge neutrality. An even simpler model involving only charge exchange and spontaneous emission had been studied before [9, 10].

Since the reduced models can be solved nearly completely by analytical means, the basic physical mechanisms and their dependence on cross sections and initial conditions can by analysed and understood. This relieves at the same time the problems caused by the above mentioned uncertainties for the cross sections. We have checked our analytical results numerically while this report was being written, and found excellent agreement between analytical and numerical solutions in every case.

As is to be expected, electron impact ionization of the alkali atom target affects the conditions for population inversion negatively. In this respect predictions based on the earlier Arizona group model were too optimistic. On the other hand the situation is much better than one would expect on the grounds of the (wrong) model of ref [6], which violates space charge neutrality. A more detailed summary is given in section 5.

Our second aim was to set the ground for more reliable calculations of cross sections. A point of concern was that the presence of intense radiation from spontaneous and stimulated

emission of the excited Helium atoms might influence the cross
sections for electron impact ionization, which was seen to be an
extremely important process. This possibility was demonstrated
before for processes involving the emission of charged particles
[11]. In fact it had been predicted recently in the literature that
the presence of intense laser fields would lead to an optically
induced band structure for charged particles [12]. Such an effect,
if present, would strongly modify the phase space available for
electrons emmitted in impact ionization, and hence affect the
ionization cross section. A careful theoretical analysis of this
problem showed that the predicted optical bandstructure is an
artifact of the non-relativistic approximation used in ref [12], and
will not be observed in reality [13].

In section 2 we shall describe the three models used in the
analysis of the pumping kinematics of a charge exchange laser. In
section 3 we discuss the solutions to the rate equations of the
models considered and the physical processes described by these
solutions. Several examples of numerical solutions are presented.
We also derive the implications of our results for a working charge
exchange pumping scheme. In section 4 we give an account of our
theoretical analysis of the "bandstructure" problem. The results
from this and the charge exchange work are finally summarized in
section 5.

II. Models of Clashing Beam Charge Exchange Reactions

In the clashing beam charge exchange a pulse of He plasma
collides with a cloud of alkali atoms (Cs) at relative velocity v
(see Figure 1).

In this situation both the positive ions and the electron in the plasma will collide with the alkali atoms. The first process leads to the desired charge exchange reaction, while the second process leads to the undesired electron impact excitation and ionization of alkali atoms. There is an important difference between these processes: while charge exchange leads to depletion of both plasma ions and alkali atoms, the ionization process leads to a buildup of electron density and a depletion of alkali atoms. On these grounds one would expect the ionization process to dominate after the plasma has penetrated into a sufficient depth of the alkali target. It is for this expected long run dominance that we consider electron impact ionization the most important competing process, and we have confined our attention to this in order to maintain a manageable kinematical model.

While our first guess about the ionization process is confirmed by the results discussed below, its full impact can only be understood when we compare these results with those from a model in which the ionization process is absent [7, 8]. In this latter model a dynamical steady state situation develops almost immediately after the colliding beams begin to overlap, a situation with has not been fully realized in the literature thus far (see Ref. 6), where it is stated that buildup of ground state helium would make inversion impossible further away from the leading edge of the alkali target. Taken as a general statement, this assertion is in variance with our solutions for the simplest kinematical model [9, 10].

A second important point about the ionization process is that the buildup of electron density is limited by plasma screening,

resulting in an overall balance of positive and negative space charges. This screening effect has to be built into the rate equations explicitly. A failure to do so will give unphysical results, since the unscreened rate equations do not conserve charge neutrality. This point was overlooked in ref. [6] (see Eq. 4e).

In the following we shall discuss three models:

a. charge exchange and spontaneous emission only,

b. charge exchange, electron impact ionization, plasma screening and spontaneous emission,

c. charge exchange, electron impact ionization with violation of charge neutrality, and spontaneous emission.

Both models a) and c) are unphysical. They are however the only models which have been treated in the literature so far, and serve to illustrate the main features of the more realistic model b).

The rate equations are as follows:

Model a)

$$\frac{\partial}{\partial y} n_+ = - n_+ N_0 \tag{1a}$$

$$\frac{\partial}{\partial x} N_0 = - n_+ N_0 \tag{1b}$$

Model b)

$$\frac{\partial}{\partial y} n_+ = - n_+ N_0 \tag{1b}$$

$$\frac{\partial}{\partial x} N_0 = - n_+ N_0 - q'(n_+ + N_+)N_0 \tag{2b}$$

$$\frac{\partial}{\partial x} N_+ = - \frac{\partial}{\partial x} N_0 \tag{3b}$$

Model c)

$$\frac{\partial}{\partial y} n_+ = - n_+ N_0 \tag{1c}$$

$$\frac{\partial}{\partial x} N_0 = - n_+ N_0 - q e_- N_0 \tag{2c}$$

$$\frac{\partial}{\partial y} e_- = q e_- N_0 \tag{3c}$$

For all models the density, n_*, of excited helium and the population inversion Δn are given by:

$$\frac{\partial}{\partial y} n_* = - n_* + n_+ N_0 \tag{4}$$

$$\frac{\partial}{\partial y} n_0 = n_* \tag{5}$$

$$\Delta n = \frac{1}{3} n_* - n_0 \tag{6}$$

Here n_+, n_* and n_0 are the densities of ionized, excited and ground state helium. The densities of neutral and ionized alkali atoms are denoted by N_0 and N_+.

The alkali target is assumed to be at rest, and the helium plasma moving in the positive y direction with velocity v.

$$x = vt - y$$

gives the position in the comoving frame of the plasma, measured from the leading edge of the plasma pulse.

Both x and y are measured in units of the decay length λ of the excited helium:

$$\lambda = v \cdot \tau_{He} = 5 \times 10^{-3} \text{ cm}$$

for

$$v = 10^7 \text{cm/sec}, \quad \tau_{He} = 5 \times 10^{-10} \text{sec}$$

The alkali density is measured in units of the density

$$\tilde{N} = (\sigma\lambda)^{-1} = 10^{17} \text{cm}^{-3}$$

for a charge exchange cross section of $\sigma = 2 \times 10^{-15} \text{ cm}^2$.

For model c) the electrons are assumed to drift freely with the same velocity v as the helium atoms and ions [Equation 3.c]. In reality however the electrons are screened over distances of the order of Debye length . For an electron density of 10^{16}cm^{-3} and

a plasma temperature of 30 eV

$$\lambda_D = 4\times10^{-5}\text{cm},$$

which is two orders of magnitude smaller than the scale of length .
We have therefore assumed strict charge neutrality in model b), and
put the electron density equal to the density of positive ions,

$$e_- = n_+ + N_+$$

in the second term of equation (2b). q and q' are the ratios of
electron ionization cross section to charge cross section; the
latter multiplied by the ratio of average thermal electron velocity
to average drift velocity. This modification is necessary, since
the electrons are confined to the interaction region in which a
steep gradient of the neutral alkali population occurs.

III. Solutions of rate equations and physical interpretation

The initial conditions for the rate equations in Sec. II are

$$n_+(x,0) = a(x) = \text{plasma pulse shape}$$

$$N_0(0,y) = b(y) = \text{alkali target shape}$$

With:

$$A(x) = \int_0^x dx'\, a(x') \qquad B(y) = \int_0^y dy'\, b(y')$$

equations (1a) and (2a) are readily solved:

$$n_+(x,y) = a(x)\, \frac{e^{A(x) - B(y)}}{1 - e^{-B(y)} + e^{A(x) - B(y)}} \tag{7}$$

$$N_0(x,y) = b(y)\, \frac{1}{1 - e^{-B(y)} + e^{A(x) - B(y)}} \tag{8}$$

Two regimes are of interest: the transient regime ($\exp(-B(y))$,
and the steady state regime ($\exp(-B(y)) \ll 1$).

In the steady state regime a well defined interaction region
develops. Steep gradients in the densities occur at the location
x_0, y_0 where

$$A(x_0) - B(y_0) = 0.$$

In this interaction region we have

$$A(x) - B(y) \simeq a(x_0)(x - x_0) - b(y_0)(y - y_0)$$

$$\tag{9}$$

to a good approximation, since the rise distances of both plasma and
alkali population are some orders of magnitude larger than the unit
of length λ .

From (9) we have

$$x - x_0 = v(t-t_0) - (y-y_0) = \frac{b(y_0)}{a(x_0)} \ (y - y_0) \ ,$$

$$y - y_0 = \frac{v \ a(x_0)}{a(x_0) + b(y_0)} \cdot (t-t_0) = v_{eff}(t-t_0), \tag{10}$$

showing that the interaction region moves at an effective velocity $v_{eff} < v$ into the alkali target. In this dynamical steady state situation the region to the left of the interaction region contains Helium plasma and alkali ions, while the region to the right contains neutral Helium and alkali atoms (see Figure 1). It is precisely this difference between effective velocity of propagation of the interaction region, and actual drift velocity of the helium plasma, which makes it necessary to explicitly account for plasma screening. Hence the positive space charge in the left region is compensated by a corresponding negative electronic charge, while no electrons penetrate into the right region.

Once the densities n_+ and N_0 are known, the density n_* and the inversion Δn are determined by 4.5 and 4.6. This is the case for models a, b, and c. We note that a steady state inversion develops for model a), if the threshold density of alkali atoms is exceeded.

In the model analysed here the buildup of ground state population will not prohibit inversion further down stream, since this population is drifting out of the interaction region at a velocity larger than the effective velocity of propagation of that region.

This situation may be different in reality, where backscattering of helium with a resulting spread in velocity

distribution will occur. The effect will be especially harmful at alkali densities just above threshold, since the inversion density is then one order of magnitude or more smaller than the densities of excited and ground state density.

Two plots of excited and inversion density illustrating the steady state kinematics are shown in Figures 2.a. and b. Helium and cesium densities are 1 and 10, and the two points of observation in the alkali target are separated by one unit of distance.

An analytical expression for the density of excited helium and inversion is obtained from 4, 5, and 6:

$$n_* = \int_0^y dy' e^{y'-y} n_+ N_0 \tag{11a}$$

$$\ddot{n}_+ + n_* + n_0 = a(x) \tag{11b}$$

$$\Delta n = \int_0^y dy' e^{y'-y} [\frac{1}{3} N_0 n_+ - (a - n_+)] \tag{11c}$$

These formulae are generally valid. Using the solutions 7) and 8) for system a), which is the most favorable if unrealistic situation (no competing processes), we derive the following necessary condition for positive inversion:

$$b(y_0) > 3 \tag{12}$$

where y_0 is the position in the alkali target at which inversion is

expected. Numerical evaluation of integral (11c) shows that b = 3 is indeed the threshold for positive inversion [8].

This result can also be understood intuitively. The rate γ at which excited helium is produced by charge exchange is given by

$$\gamma = v \cdot \sigma \cdot N_0$$

For inversion to occur γ must be larger than the decay rate:

$$\gamma > \tau^{-1} \quad , \qquad \text{hence} \qquad N_+ > \frac{1}{v\sigma\tau} = \tilde{N} \quad ,$$

and $N_0 > 1$ in the units defined above.

Inversion densities in the steady state regime are typically one order of magnitude less than the helium plasma density in the pulse at the location defined by the interaction region [7].

In the transient regime inversion is always achieved as long as the helium has not penetrated more than about a decay length into the alkali target. However, inversion densities will be several orders of magnitude less than in the steady state. This is most easily seen in the limit were the penetration depth is about an order of magnitude less than the decay length.

By approximating the exponential in (11a) by unity we obtain:

$$n_*(x,y) \simeq a(x) - n_+(x,y) \tag{13}$$

$$\Delta(x,y) \simeq \frac{1}{3} n_*(x,y)$$

$$\Delta(x,y) = \frac{1}{3} a(x) \frac{(e^{B(y)} - 1)e^{-A(x)}}{1 + (e^{B(y)} - 1)e^{-A(x)}}$$

$$\simeq \frac{1}{3} B(y)a(x)e^{-A(x)}$$

(14)

where the last approximation holds for $B(y) \ll 1$. Since we assumed the penetration depth to be of the order 10^{-3} cm, this assumption will always hold for realistic alkali targets.

In the Arizona experiments ([5],[7]) alkali targets with peak density of $10^{16} - 10^{17}$ cm^{-3} were created by flashlamp evaporation of cesium films. The leading edge of these targets is well described by the distribution

$$N_0(\mu) = N_0 \mu^5 e^{-\mu^2}$$

with a target width of $\Delta\mu \simeq 1 \simeq 1$ cm. In units of the decay length the leading edge is thus given by

$$N_0(y) \simeq N_0 \, 10^{-10} y^5 .$$

This example demonstrates the significant reduction in inversion density in the transient regime as compared to the steady state regime.

The effects of electron impact ionization in the realistic, screened model b) modify the situation described above in some quantitative aspects. The main features, like existence of a

transient regime without threshold and a steady state regime with non-zero inversion threshold, are the same.

The analytical treatment of model b) is quite complex, and will not be given here. Instead we describe its features in qualitative terms, and present some computer results for illustration.

Since plasma screening confines the electrons to regions of positive space charge, a well defined interaction region develops with no free electrons ahead of that region. Within that region screening also prevents an excessive buildup of electrons, and electrons are left behind with the ionized alkali rarget, as the interaction region moves on. The net effect is a reduction the effective alkali density available for charge exchange. Figures 3 a) and 3 b) show excited Helium and inversion density, for a system without and with electron impact ionization. The reduction of effective alkali density is apparent in the higher effective velocity of the interaction region and the smaller gain. Figure 4 shows the much reduced consumption of Helium plasma (curve b) for the case of model b) as compared to model a) (curve a).

The unrealistic model c) of the pumping kinematics studied in Ref. 6 shows qualitatively different features. Due to the free propagation of electrons, the electron density builds up exponentially by ionization, and no steady state inversion exists. Population inversion occurs only in the leading edge of the alkali target, and the situation there is quite similar to the situation discussed above for model c.

Analytical solutions showing this behavior can be constructed explicitely for certain values of relative cross section q'. For q'

= 1 the helium and electron density are given by

$$n_+(x,y) = a(x) \frac{e^{B(y)} \sinh A(x) + \cosh A(x)}{e^{B(y)} \cosh A(x) + \sinh A(x)}$$

$$e_-(x,y) = a(x) \frac{e^{B(y)} \cosh A(x) + \sinh A(x)}{e^{B(y)} \sinh A(x) + \cosh A(x)}$$

$$\simeq a(x) e^{B(y)} \quad \text{for} \quad e^{-A(x)} \ll 1.$$

The nearly instantaneous depletion of the alkali target due to the ionizing electron avalanche in this model is shown in Figure 5 (curve c). Curves a and b show the alkali depletion as the interaction region passes by for models a and b.

Figure 6 shows the violation of charge neutrality for model c with excess electron density in the leading edge of the plasma pulse, and excess ion density in the tail.

It is apparent from this that previous evaluation of the charge exchange pumping scheme based on an extensions of model c [6] underestimated the potential of this scheme. While population inversion in the leading edge of the alkali target is common to all models studied here, the realistic, screened model b) proposed here shows that at sufficient depth in the target a steady state kinematics with well defined interaction region develops.

For alkali densities of about $10^{18} cm^3$ a steady state inversion develops. Inversion densities in this regime exceed the transient inversion densities by several orders of magnitude.

4. Electronic wavefunctions in an intense radiation field

Intense radiation fields as those generated by spontaneous and stimulated emission in a charge exchange laser modify the electronic states considerably, and can greatly influence cross sections for collision and other processes involving charged particles [11]. For example in an ionizing collision between an electron and an alkali atom the ejected photo-electron will be accelerated by the radiation field. The corresponding shift the in final electron energy and the modification of the density of final states will then increase the cross section for that collision.

While exact relativistic wave functions for electrons in a plane-wave-radiation field have been known for a long time [14, 15], their application to a nonrelativistic calculation of ionization cross section is not straight forward. It is therefore desirable to have an independent formulation in terms of the nonrelativistic quantum mechanics. Such an analysis was attempted recently in Ref. 12. These authors predicted the existence of a spectrum of discrete nonrelativistic energy levels whose level-separations are in the microwave region.

Such an optically induced band structure would make it necessary to recalculate ionization cross sections by using the appropriate electronic wavefunctions, which in this case are given by nontrivial solutions of Mathieu's equation [13].

In a careful analysis of this problem [13] it was shown that the results of ref [12] are an artefact. This artefact results as a consequence of the nonrelativistic approximation, if the field intensities are high enough to accelerate electrons to relativistic

velocities. A correct treatment of the nonrelativistic theory was given, and it was shown that the WKB approximation is valid throughout the nonrelativistic regime. As a consequence the influence of the radiation field an ionization cross sections is relatively easy to assess, and may be neglected for field intensities in the nonrelativistic regime. We refer to the enclosed manuscript for details.

5. Summary and conclusion

We have studied two simplified models of the pumping kinetics in a clashing beam charge exchange laser. The first model includes electron impact ionization and plasma screening, and is a realistic description of the actual situation. To the best of our knowledge this model has not been studied before. The second model does not include plasma screening. It violates charge neutrality, and is hence not a realistic description. An extension of this model was studied numerically before [6].

Our analysis uses scaling laws to absorb all numerical parameters like charge exchange and ionization cross section into suitably chosen units of length, time and densities. Its qualitative results, therefore, remain unchanged, and quantitative results are easily adapted should the values of some of these parameters have to be modified [8].

Both models show transient population inversion in the leading edge of the alkali target. The inversion densities here are several orders of magnitude below the plasma density.

The most promising feature of the first, realistic model is the existence of a steady state regime. In this regime steady state

inversions can be achieved, if the target densities exceed a threshold of about 10^{18} cm^{-3}.

The inversion densities which can be obtained in this regime are comparable to the plasma densities, and are, hence, several orders of magnitude larger than the transient inversion densities.

On the other hand the unrealistic, unscreened model, which is the only one analysed to some extent in the literature so far [6], does not exhibit a steady state regime. This is due to the exponential buildup of the freely drifting electron population, which rapidly depletes the alkali target.

We conclude that the prospects of the charge exchange pumping scheme are much better than has been expected before. Total VUV output and gain in the steady state regime will be orders of magnitude larger than in the transient regime studied so far.

At an inversion density of 5 x 10^{15}cm^{-3} for example the gain would be

$$g \simeq 1.85 \times 10^2 \text{ cm}^{-1} .$$

The target threshold densities in the steady state regime are of the order of 10^{18} cm^{-3}. Cesium densities close to 10^{17} cm^{-3} have been achieved in the Arizona experiments [5, 9]. With further progress in Cesium evaporation technology operation of a charge exchange laser in the steady state regime seems to be a realistic possibility.

The influence of the intense radiation fields present in such lasers on relevant collisional cross sections was also addressed.

It was shown how the correct electronic states can be obtained in the nonrelativistic approximation, and the existing misconceptions about this point in the literature were corrected. This work lays the ground for a more careful evaluation of the relevant cross sections.
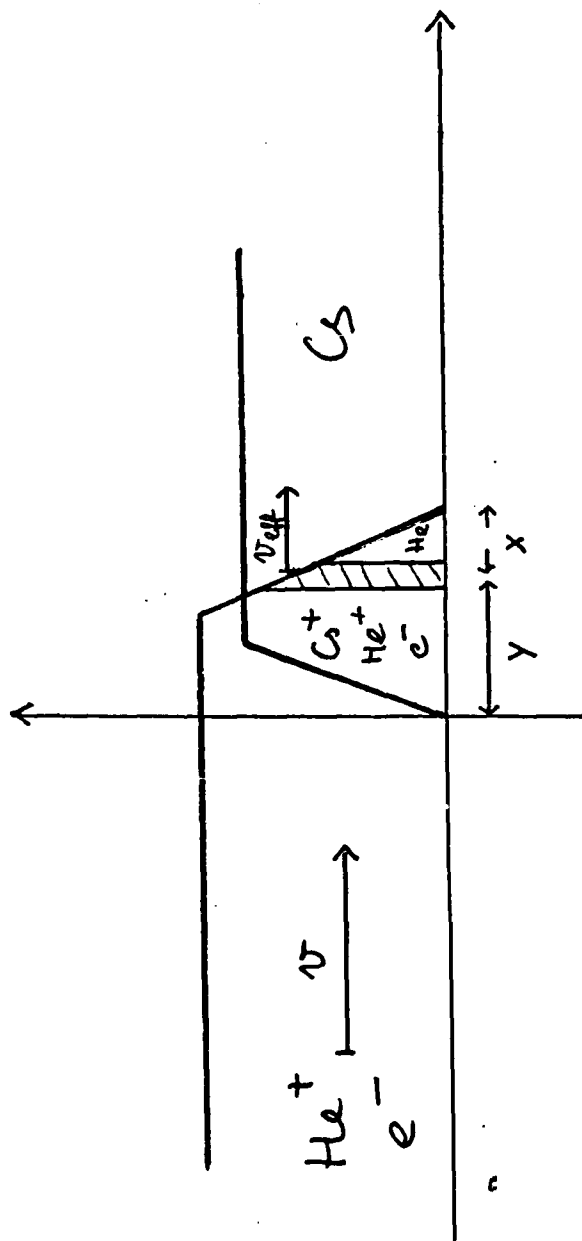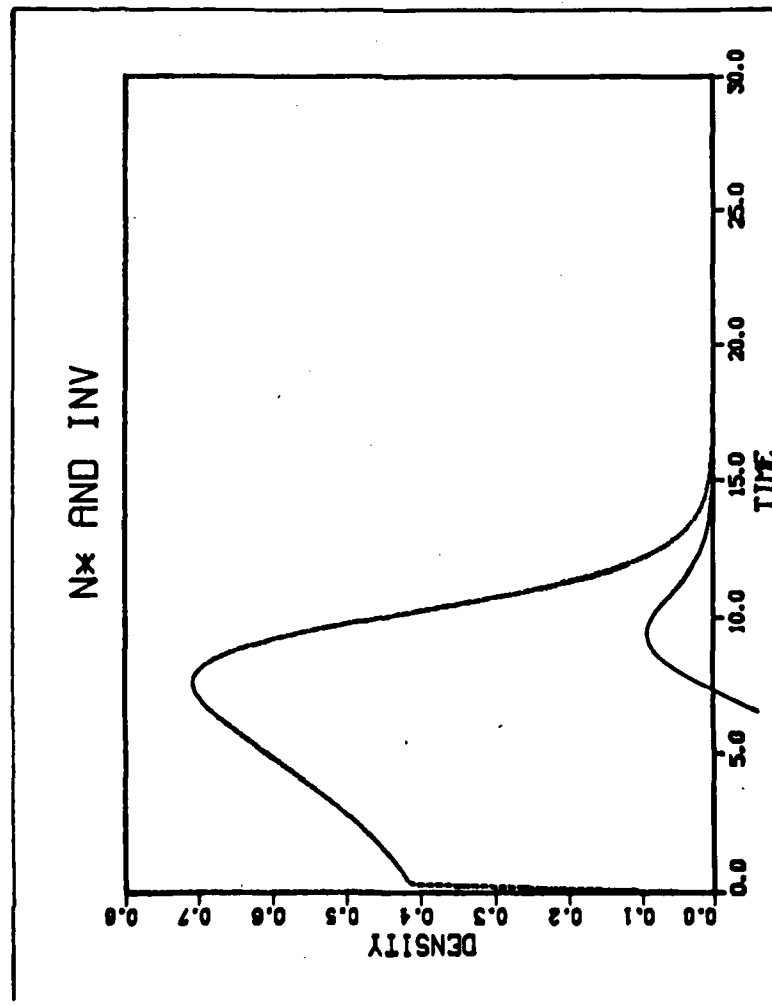
Fig. 1 Sketch of collision kinematics and coordinates.

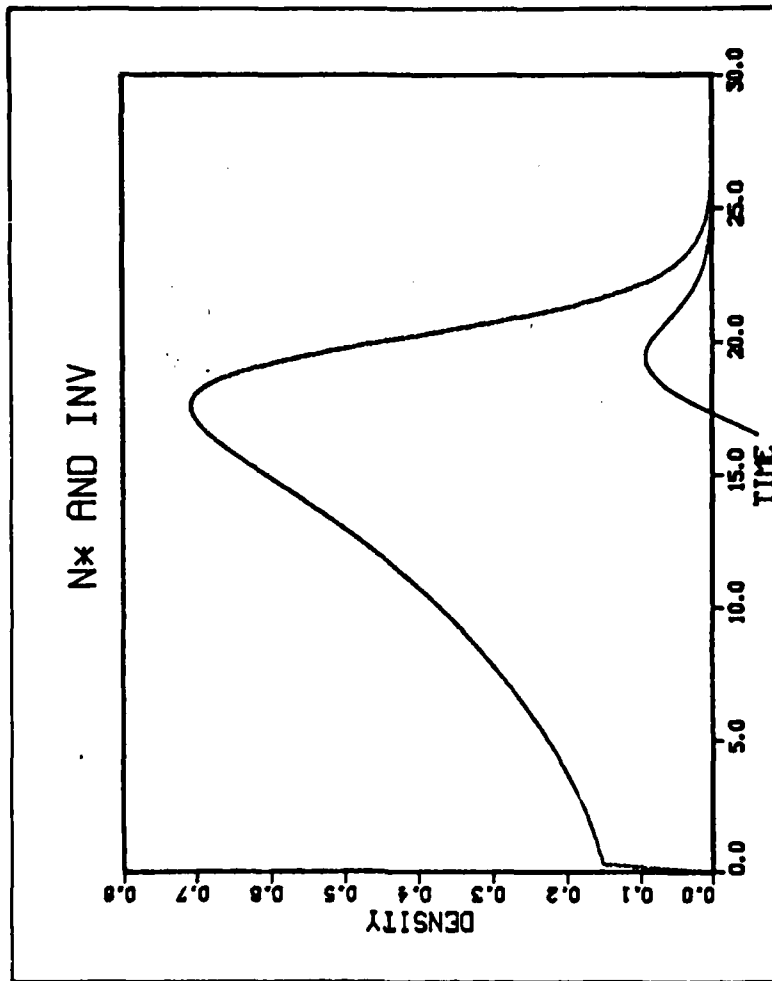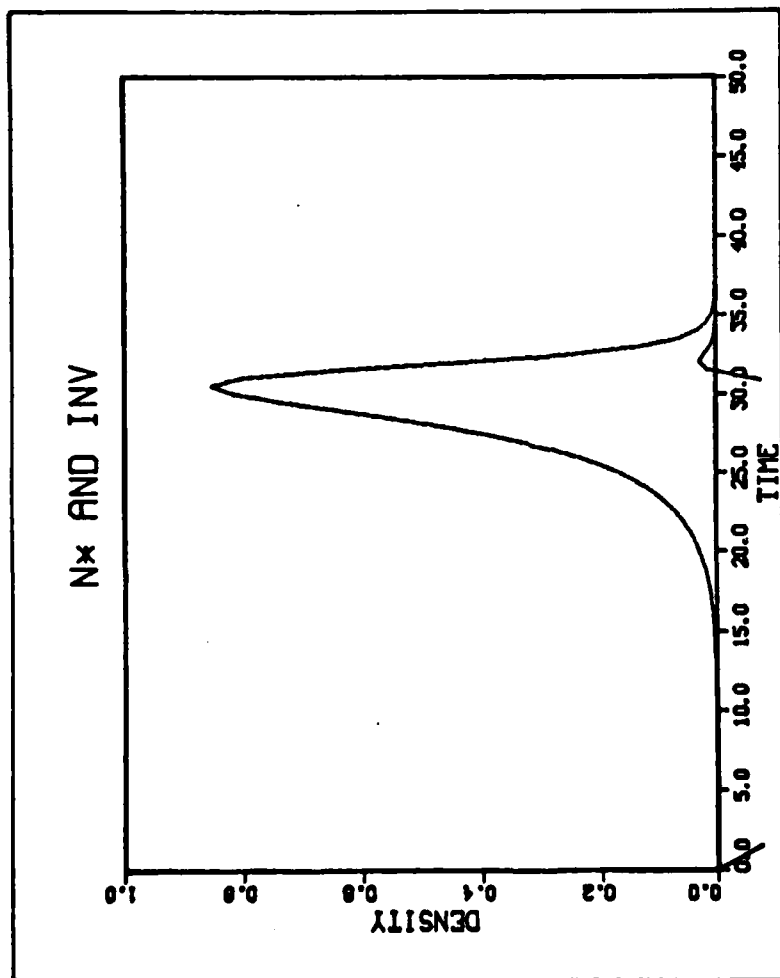22

Fig. 2a and 2b Steady state inversion at helium density $n_+ = 1$ and alkali density $N_0 = 10$ as calculated with model a. Points of observation are one unit (decay length) apart.
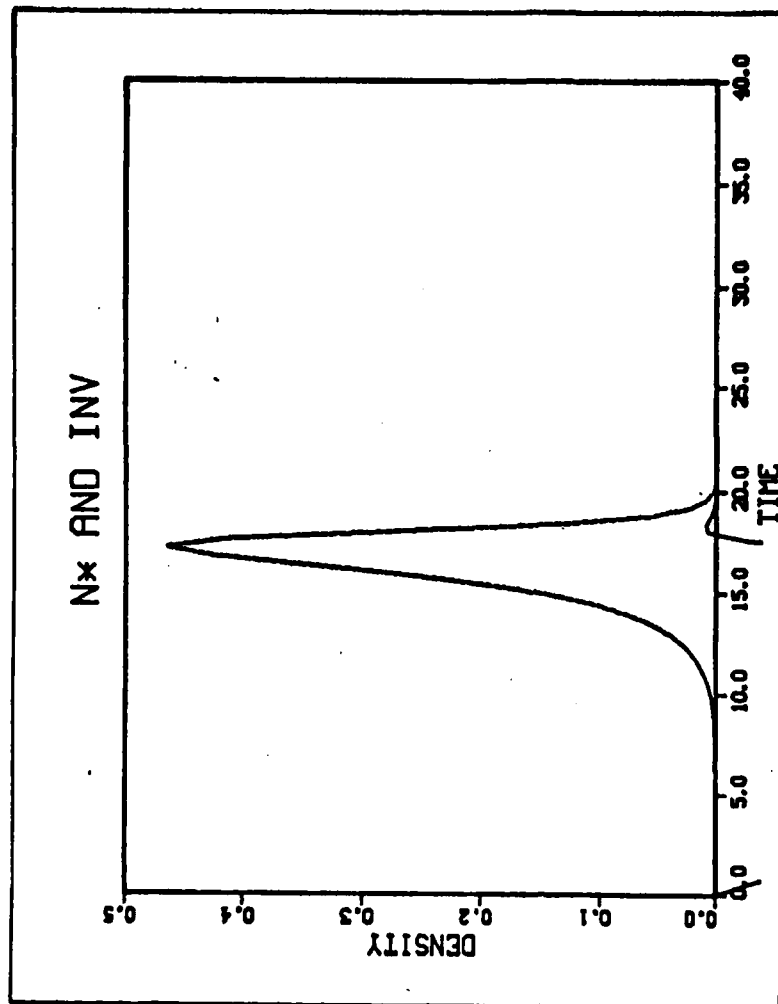
Fig. 3a and 3b Excited helium and inversion densities for model a)

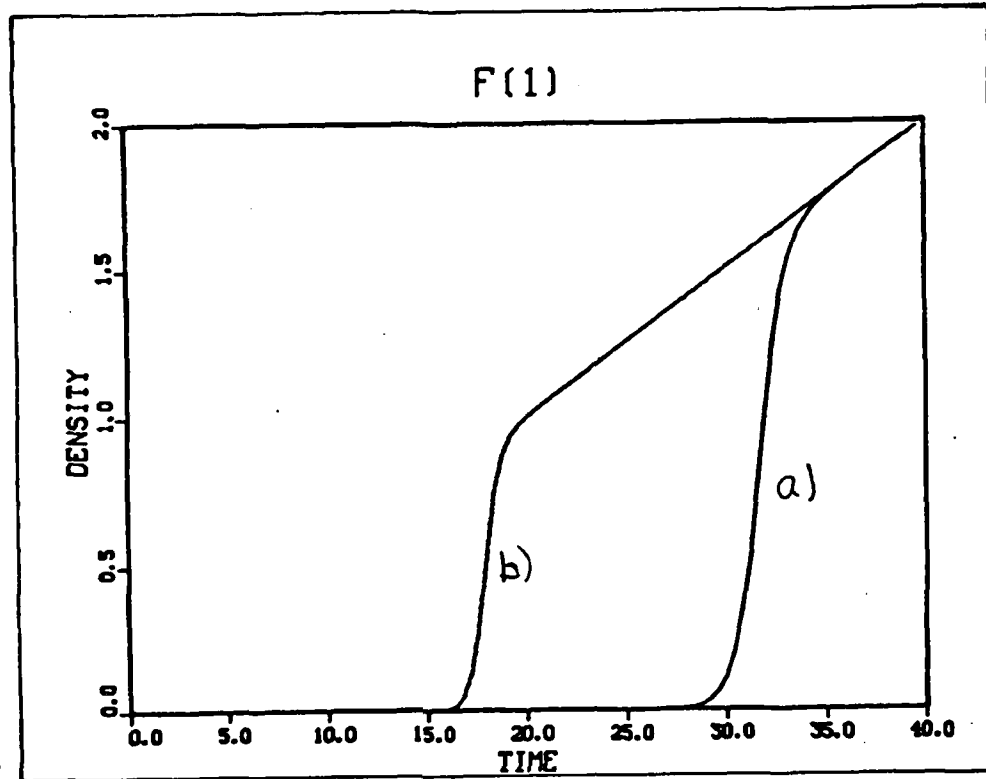(without ionization) and model b) (with ionization,

$q' = 0.3$).

Fig. 4 Reduced plasma depletion (curve b) for through electron
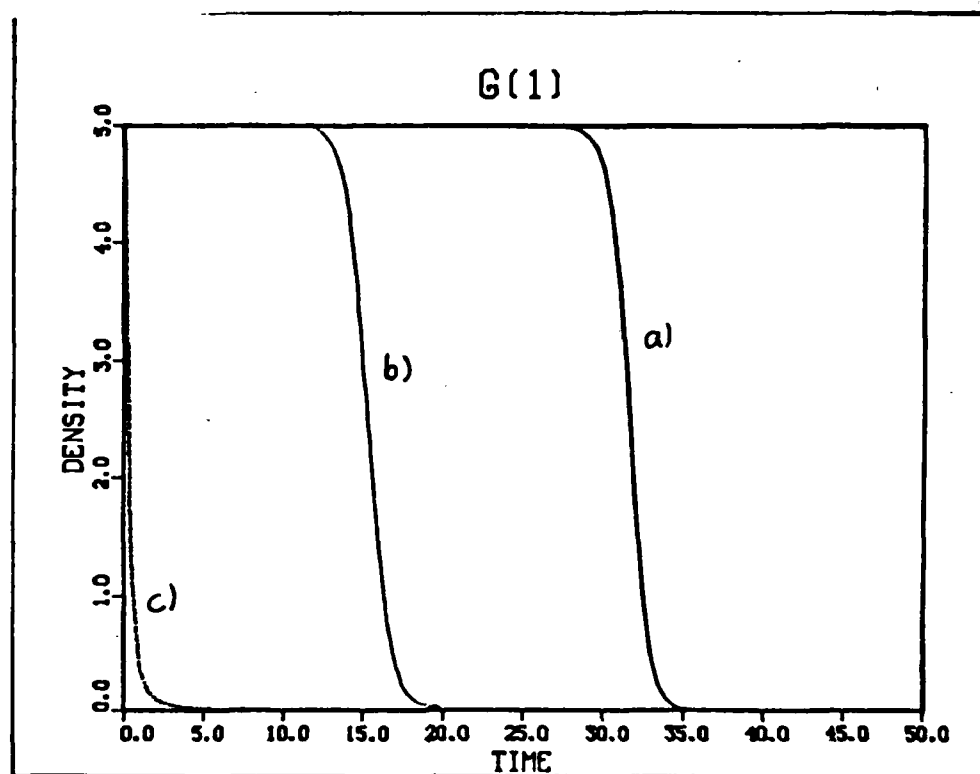impact ionization.

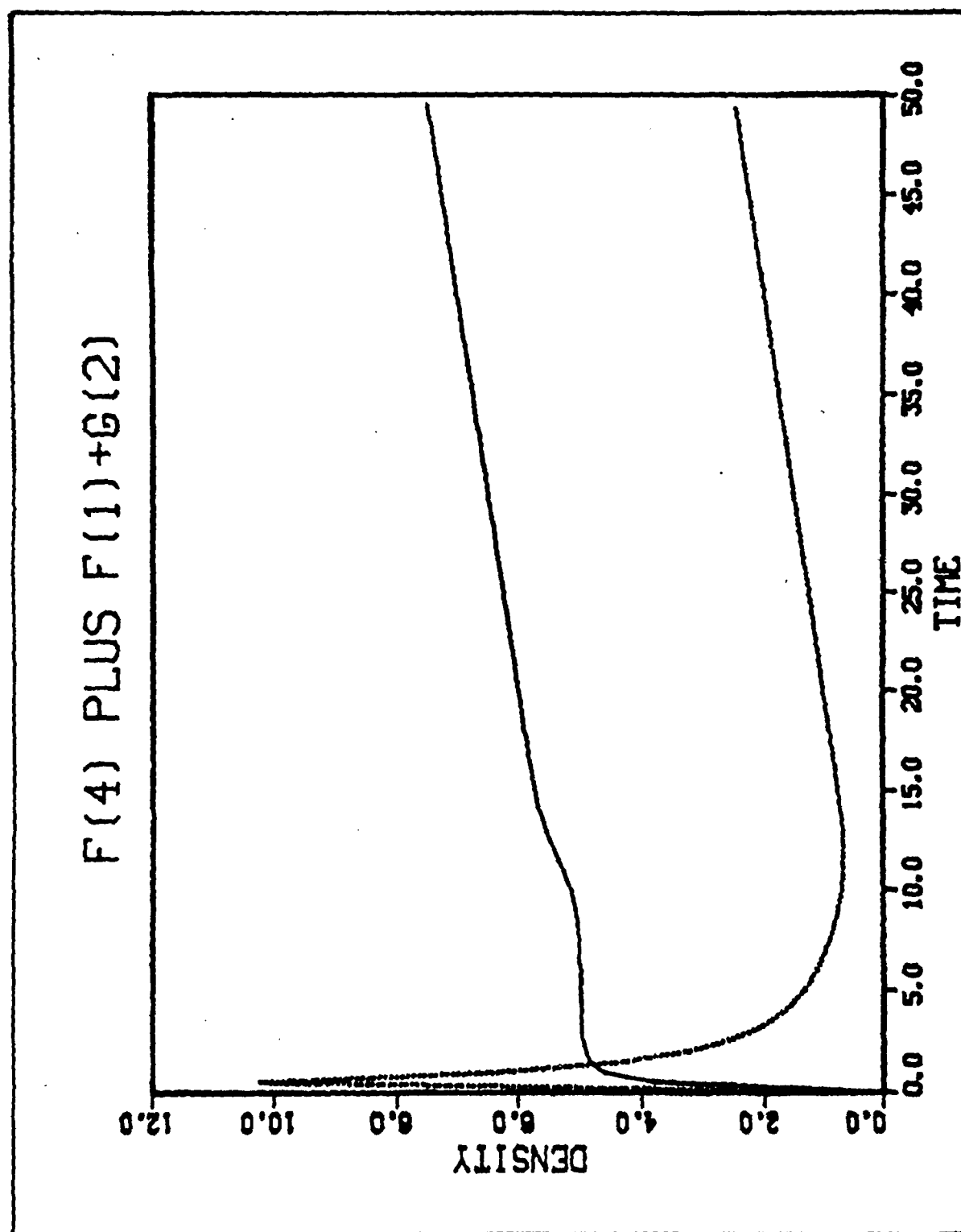Fig. 5 Cesium depletion for model a), b), and c).

Fig. 6 Space charges in model c). Dotted line, electrons, solid

line: positive ions.

For Figs. 3 through 6 linear rising pulse shapes were assumed with maximal intensity and ramp length of 5 and 100 for the plasma pulse and 5 and 10 for the alkali target. The point of observation is at position y = 10 in the target. Units of length and density are defined in the test. Approximate values are

$$\tilde{y} = 5 \times 10^{-3} cm; \qquad \tilde{N} = 10^{18} cm^{-3}$$

References

1. J. W. McGrowan, R. I. Stebbings; Appl. Opt. (Suppl 2) 68-72, (1965).

2. L. P. Presnyakov, V. P. Shevel'ko, JETP Lett. 13, 203-204 (1971).

3. M. O. Scully, W. H. Louisell, W. B. McKnight, Opt. Comm 9, 246-248 (1973).

4. H. Mahr, M. Roeder, Opt. Comm. 10, 227-228, (1976).

5. D. Anderson, J. McCullen, M. O. Scully, J. F. Seely, Opt. Comm. 17, 226-230 (1976).

6. D. A. Copeland, H. Mahr, C. L. Tang, IEEE Journ. QE-12, 665-673 (1976).

7. R. E. Olson, F. T. Smith, Phys. Rev. A7, 1529 (1973).

8. C. Reymond, J. Pommier, Vu Ngoc Tuan, M. Barat, Phys. Rev. Lett. 43, 579 (1979).

9. "Theoretical analysis of a charge-exchange He-Cs laser". The Arizona group, Optical Sciences Center, University of Arizona (1976), unpublished report.

10. "Analysis of VUV and soft X-ray lasing based on charge exchange mechanisms", J. C. Bellum, W. W. Chow, K. Druhl, M. O. Scully, paper presented at the Topical Meeting on laser techniques for extreme ultraviolet spectroscopy, Boulder 1982.

11. W. Becker, W. H. Louisell, J. D. McCullen, M. O. Scully, Phys. Rev. Lett. 47, (1981).1262.

12. J. Bergou, S. Vant, J. Phys. A14, 2281 (1981).

13. K. Druhl, J. McIver, "Charged particles in an intense, plane electromagnetic wave: limitations of the nonrelativistic theory". Journ. Math. Phys. (in press).

4 -

DT